



ACCURATE STARTUP TECHNIQUES IN A SENSORLESS FIELD-ORIENTED-CONTROL BLDC (SINUSOIDAL) MOTOR DRIVER

By Vashist Bist and Shashank Wekhande,
AvantGarde Solutions Pvt. Ltd.,
Consultants to Allegro MicroSystems

INTRODUCTION

Allegro's QuietMotion family of motor drivers integrates field-oriented-control (FOC) algorithms that provide a code-free environment for designers to achieve the best efficiency and acoustic performance. These algorithms allow for smooth, quiet motion, significantly reducing the research and development (R&D) expenses for code development and reduces time to market.

The AMT49406 is the first 50 V, 3-phase sensorless, brushless DC (BLDC) motor (sinusoidal) or permanent magnet synchronous motor (PMSM) gate driver from the Allegro QuietMotion™ family. This device is fully-integrated with FOC (Allegro's proprietary windowless sinusoidal algorithm) and advanced features, such as soft-on and soft-off (SOSO) and proprietary nonreverse fast-startup 2-pulse initial position detect (IPD)) algorithms.

Achieving fast and accurate startup with the sensorless control of the PMSM is a key challenge faced by designers. The overall startup procedure can be divided into two

subcategories of the initial position detection/alignment and the open-loop startup. The rotor position is either aligned to a known position by applying a high current for a specified duration or the rotor position is detected using IPD techniques. Once the rotor position is aligned (or detected), open-loop pulses of increasing frequency are applied to the motor such that the rotor begins to rotate. When the rotor has achieved enough speed that back electromotive force (EMF) can be detected, the control mechanism is shifted to the sensorless mode.

This application note presents various startup techniques available for use with the AMT49406 device. A detailed description of four startup modes—Align and Go, 6-Pulse IPD, 2-Pulse IPD, and Slight-Move—is presented in this application note. For each startup mode, application-specific descriptions, key benefits, and limitations are explained. Also presented is an overview of the configurations of various startup parameters in the AMT49406 device and the details on the graphical user interface.

STARTUP MODES

AMT49406 device provides four modes of startup as described in this section.

Align and Go

This mode is the conventional mode of starting where the rotor is aligned to a fixed position (alignment) and open-loop pulses of increasing frequency are applied to the stator of a BLDC motor to increase the speed enough for proper detection of the back-EMF:

- For high-inertia motors, the acceleration parameter is set low, such that the rotor can pick up speed.
- For lower inertia motors, the acceleration can be increased to reduce the overall startup time.

The main advantage of this startup mode is the simplicity and lack of dependence on motor parameters, such as motor resistance or inductance. However, due to position alignment, the rotor can move in either direction. Therefore, this startup mode is used for applications where features like zero reverse rotation are not needed and where the startup time is not critical, such as in air purifiers.

The Align and Go startup waveforms of the AMT49406 device presented in Figure 1 show that the rotor quickly aligns to a known position (initial peak current) as open-loop pulses of increasing frequency are applied.

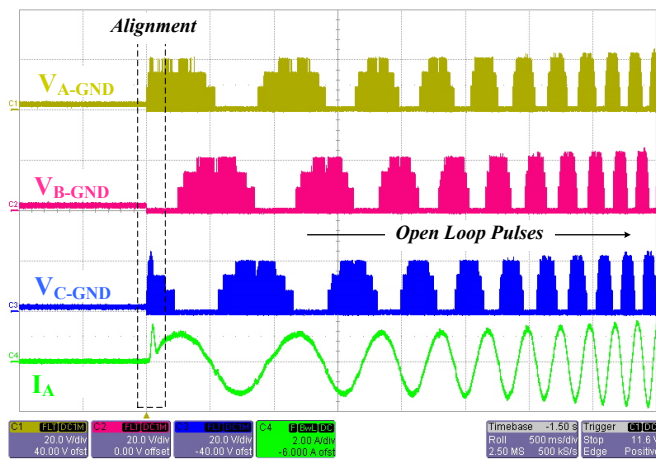


Figure 1: Align and Go Startup Waveforms

6-Pulse Initial Position Detection

The IPD algorithm is designed to detect the rotor position without any movement of the rotor, for applications where reverse rotation of the BLDC motor is not acceptable, such as ceiling or pedestal fans.

The total startup time for the IPD mode is less than the align and go mode because the align functionality is not required—only open-loop starting pulses are applied. However, the 6-pulse IPD can generate audible noise, which needs to be considered and evaluated before the final selection of the startup procedure.

The principle of operation of IPD lies in the fact that the inductance of the motor varies as a function of the rotor position. The IPD algorithm injects a small duration of current pulse to the motor; this current is not enough to overcome the inertia of rotor, so the rotor movement is not observed.

In the 6-pulse IPD algorithm, the two phases of the BLDC motor are sequentially excited such that all six combinations of the phases—AB, BA, BC, CB, CA, and AC—are excited sequentially, as shown in Table 1.

Table 1: Sequential Order of 6-Pulse IPD

Code	Phase A	Phase B	Phase C
AB	High	Low	Floating
BA	Low	High	Floating
BC	Floating	High	Low
CB	Floating	Low	High
CA	Low	Floating	High
AC	High	Floating	Low

The phase current is monitored, and the phase excitation is stopped as soon as the current reaches a set programmable threshold (i.e., the IPD current threshold). The duration from phase excitation to attainment of the current limit is noted, then the device moves on to the next sequence. This IPD time varies as a function of the inductance in the motor windings. If the permanent magnet flux is in the same direction as the generated magnetic flux, then the inductive saturation is reached earlier. Hence, the time to reach the IPD current threshold is minimized. The 6-pulse IPD phase sequencing pulse, MOSFET gate signals, and DC link current are shown in Figure 2.

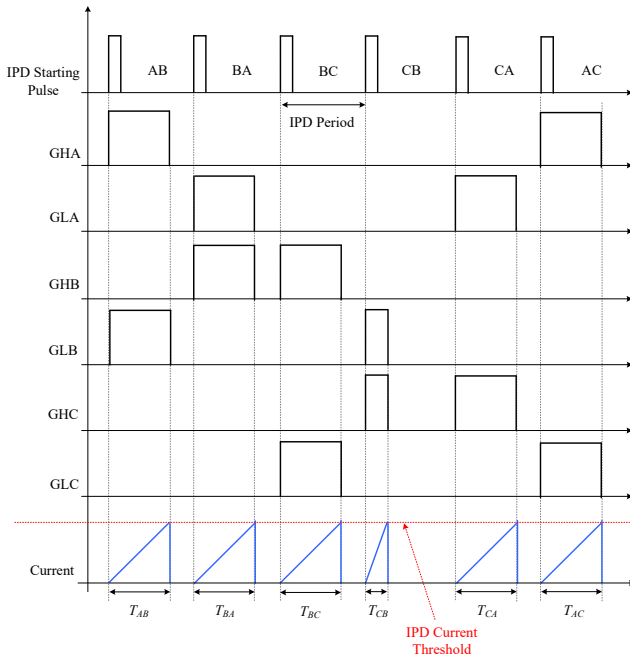


Figure 2: 6-Pulse IPD Phase Sequencing

The AMT49406 device provides an adaptive current decay to quickly reduce the current to zero: The device saves the decay time and uses it to minimize IPD detection time. The drive stage shown in Figure 3 presents the high-side MOSFET (S1) of Phase A and low-side MOSFET (S4) of Phase B in the powered state. In decay Stage 1—i.e., the coasting mode—both phases are powered off, and the current decays through the body diodes of S2 and S3, as shown in Figure 4. This will cause the inductive energy to transfer to the DC link capacitor (C_{dc}) and voltage V_{bb} will increase. Once the phase current is within the safe current limit—i.e., I_{LIM} (the MOSFET's current rating)—the low-side MOSFETs of the bridge are turned on to realize the braking stage, as shown in Figure 5. The phase current in the three different modes—driving, coasting, and braking, respectively—is shown in Figure 6.

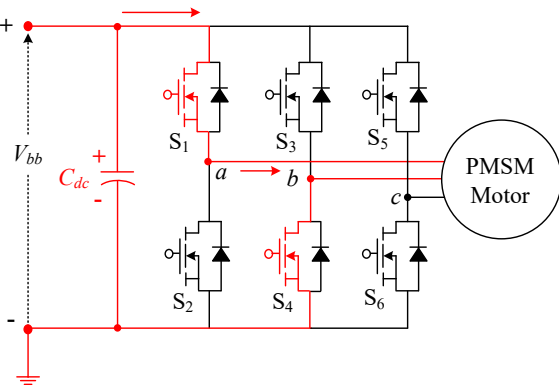


Figure 3: Drive Stage

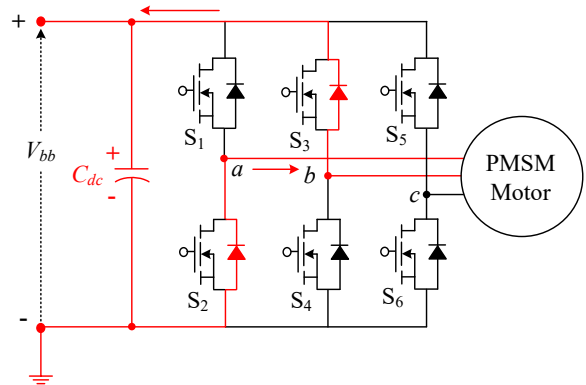


Figure 4: Decay Stage 1 (Coasting)

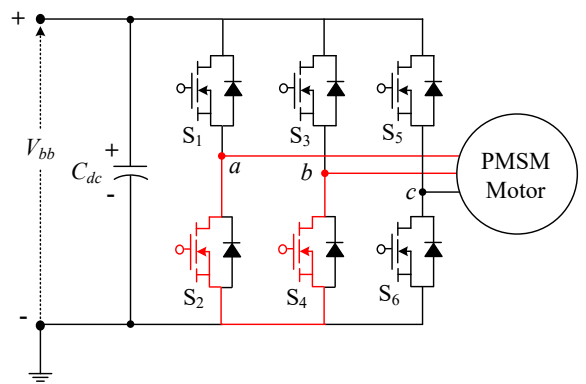


Figure 5: Decay Stage 2 (Braking)

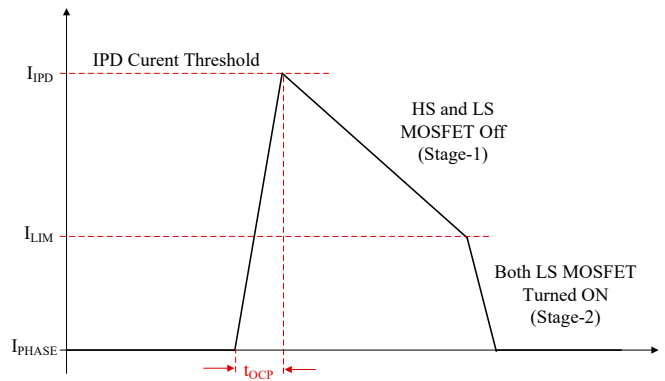


Figure 6: Decay Current

The oscilloscope waveforms of the 6-pulse IPD algorithm showing the input DC link current and the phase current are shown in Figure 7 and Figure 8, respectively. As shown in these figures, the phase current reaches the set IPD current threshold when the corresponding phase combination is excited. The decay of the current can be clearly seen in two different stages of coasting and braking. The AMT49406 device determines which of these six current pulses reached the IPD current threshold first, thus detecting rotor position.

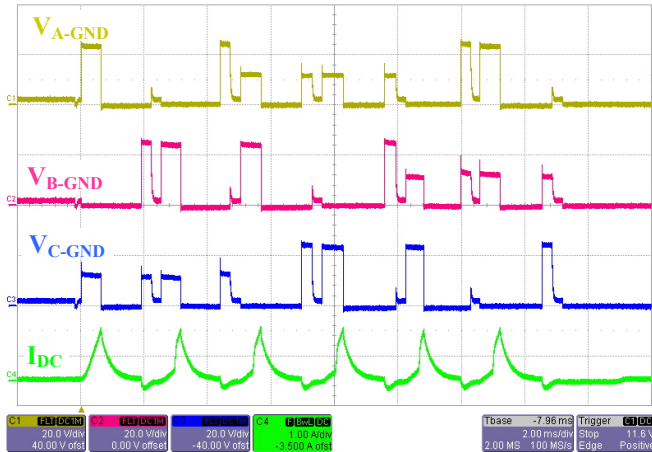


Figure 7: 6-Pulse IPD Waveforms (with DC Link Current)

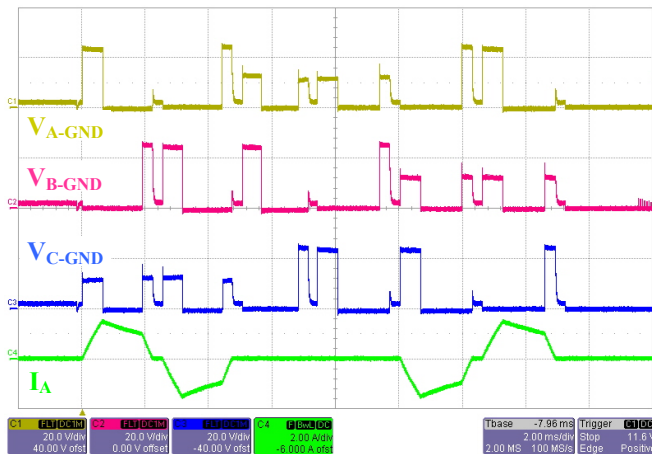


Figure 8: 6-Pulse IPD Waveforms (with Phase A Current)

2-Pulse IPD

Another method of initial position detection is the 2-pulse IPD technique. This method comprises two stages: complimentary drive and detect (CDD); and 2-polar axis current injection (PACI).

CDD Stage

The CDD stage involves a complimentary and balanced (50% duty) switching of two phases in a sequential order of phases, such as AB, BC, and AC. During these sequences, the floating phase voltage is monitored to detect the variation of inductance. The 50% duty ensures that the average voltage applied is zero and that there is no residual voltage that can lead to rotor movement in multiple such pulse width modulation (PWM) cycles. A mathematical expression of the CDD stage is presented next.

When two phases are excited (e.g., Phase AB), current flows from V_{bb} to Phase A to Phase B, then sinks to GND, as shown in Figure 9.

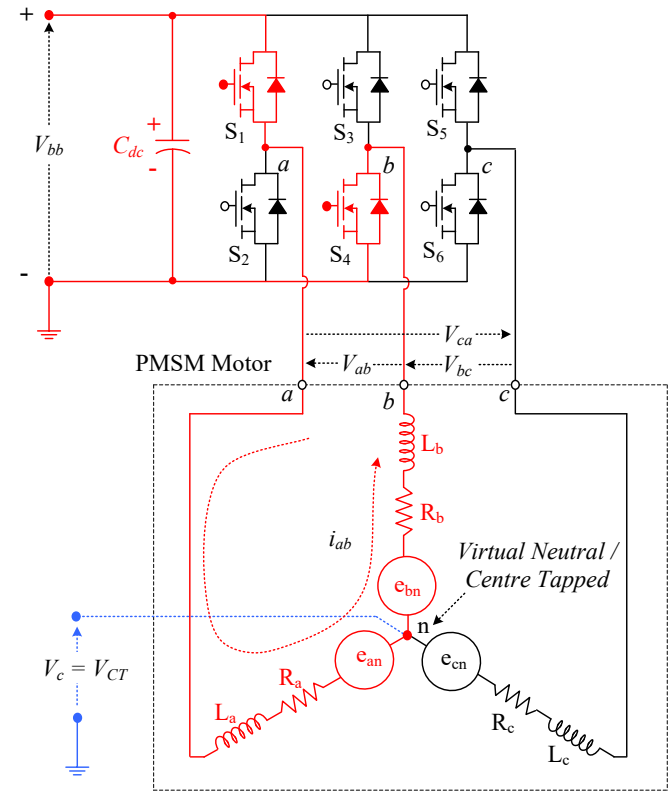


Figure 9: PMSM Motor Modeling

Phase C is a nonconducting phase. Hence, in Phase C, the floating voltage, i.e. V_{CT} (center-tapped voltage), is calculated from Phase A as:

Equation 1:

$$V_{CT} = V_{bb} - i_{ab} \times R_a - L_a \frac{d}{dt} (i_{ab}) - e_{an}.$$

Moreover, the voltage, V_{CT} , is calculated from Phase B as:

Equation 2:

$$V_{CT} = i_{ab} \times R_b + L_b \frac{d}{dt} (i_{ab}) - e_{bn}.$$

Because the rotor is not moving in this detection, the back-EMF (e_{an} and e_{bn}) is zero. Hence, Equation 1 and Equation 2 can be rewritten as:

Equation 3:

$$V_{CT} = V_{bb} - i_{ab} \times R_a - L_a \frac{d}{dt} (i_{ab}); \text{ and}$$

Equation 4:

$$V_{CT} = i_{ab} \times R_b + L_b \frac{d}{dt} (i_{ab}).$$

By adding Equation 3 and Equation 4 and rearranging, the voltage at floating Phase C (V_C) is written as:

Equation 5:

$$V_C = V_{CT} = \frac{V_{bb}}{2} + \frac{i_{ab}}{2} \times (R_b - R_a) + \frac{(L_b - L_a)}{2} \frac{d}{dt} (i_{ab}).$$

Considering a balanced BLDC motor, such that the phase resistances are equal ($R_a = R_b$), Equation 5 is rewritten as:

Equation 6:

$$V_C = \frac{V_{bb}}{2} + \frac{(L_b - L_a)}{2} \frac{d}{dt} (i_{ab}).$$

Hence, the floating phase voltage is dependent on the variation of the inductance (L_a and L_b). Therefore, it can be observed that:

Equation 7:

$$\text{if } L_b > L_a \Rightarrow V_C > \frac{V_{bb}}{2} \parallel L_b < L_a \Rightarrow V_C < \frac{V_{bb}}{2}.$$

This floating voltage (V_C) needs to be compared with the $V_{bb}/2$ voltage reference level to compare the inductances of two phases, as shown in Figure 10.

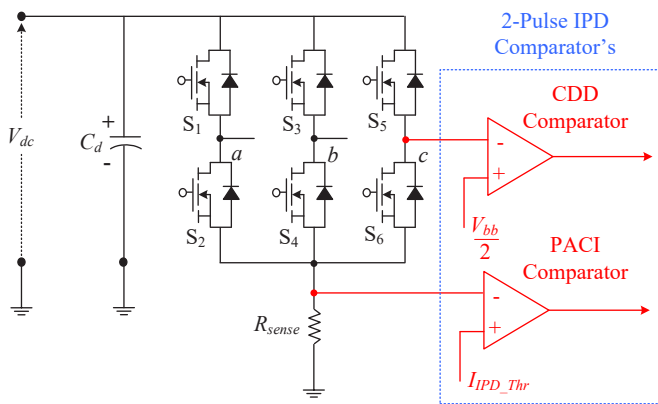


Figure 10: Comparators in 2-Pulse IPD

The 2-pulse IPD waveforms in the CCD stage are shown in Figure 11, where Phase C (blue), which is the floating phase, shows the back-EMF (i.e., V_{CT}) pulsating between levels above and below the $V_{bb}/2$ level.

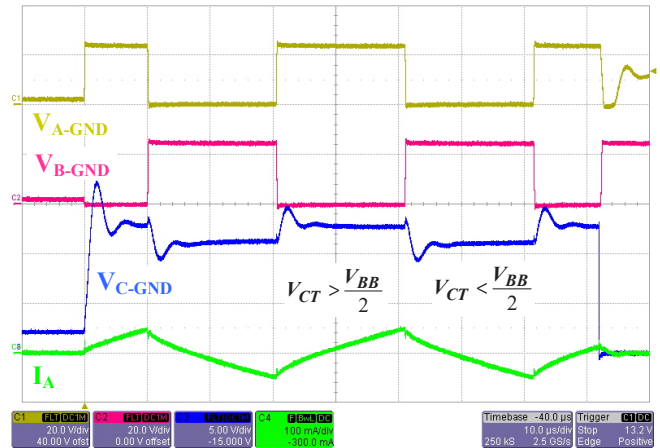


Figure 11: 2-Pulse IPD Waveforms (CDD)

In this way, the rotor position is detected in one of the sectors of the quadrant pairs, as shown in Figure 12, which includes an example of the CDD with the quadrant information. In this figure, if Phase AB is excited with complimentary pulses, the CDD algorithm will detect if the rotor lies in either Quadrant II or Quadrant III.

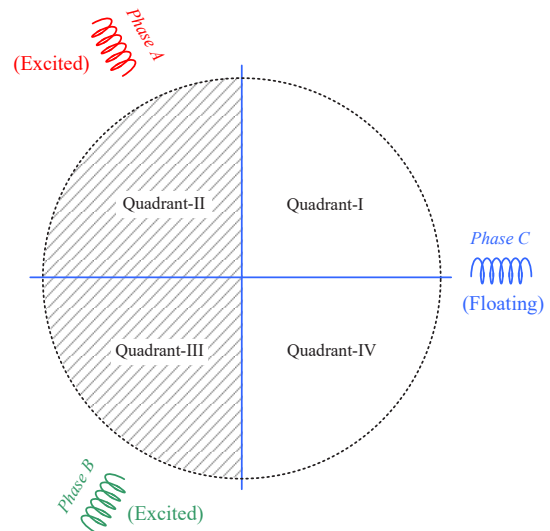


Figure 12: CDD Quadrant Pairs

In a similar way, Phases AC and BC are excited sequentially and the rotor position can be located in two of the 12 sectors, as shown in Figure 13. These 12 sectors are formed by three quadrants offset by 120 degrees. Based on the three sequential phases and the outcome of the floating phase voltage (0 when $V_{CT} < V_{bb}/2$; 1 when $V_{CT} > V_{bb}/2$), the rotor position can be determined using the lookup table, as shown in Table 2. This will determine that the rotor is aligned in either of the two angles. For the example in Figure 13, the rotor is aligned in either Sector S0 or Sector S6.

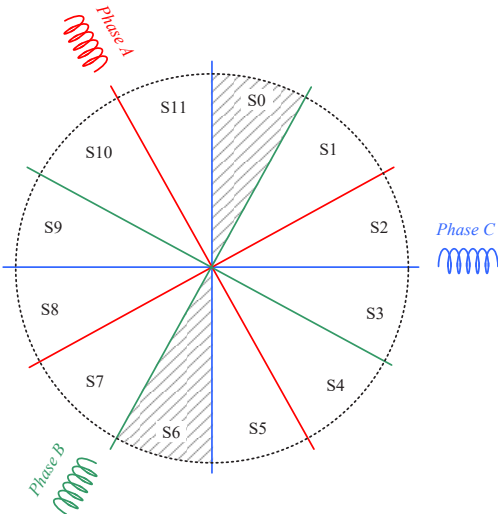


Figure 13: Two-Sector Detection From CDD Stage

Table 2: Angle of Alignment With Code

Code	Angle
001	30 or 210
011	60 or 240
010	90 or 270
110	120 or 300
100	150 or 330
101	180 or 0

PACI Stage

Once CDD is complete, the PACI is used to determine which of the two sectors identified in CDD contains the rotor. In this example, the phase current is driven in the first direction until the V_{bb} current reaches a PACI threshold. The time for V_{bb} current to reach the PACI threshold is measured. Then, in the second pulse, a current is applied in the opposite direction, and the time is noted. The shorter duration corresponds to the sector where the north pole is aligned to the corresponding phase.

The 2-pulse IPD waveforms depicting the CDD stage and the PACI stage with the DC link current and the phase current are shown in Figure 14 and Figure 15, respectively. As shown in the figures, CDD is a high-frequency stage, so the CDD stage takes much less time than the PACI stage. The PACI stage shows two current excitations—i.e., Phase CA and Phase AC, respectively—based on the corresponding sectors detected in the CDD stage. The time duration for Phase AC is shorter, thus the rotor is aligned in Phase AC.

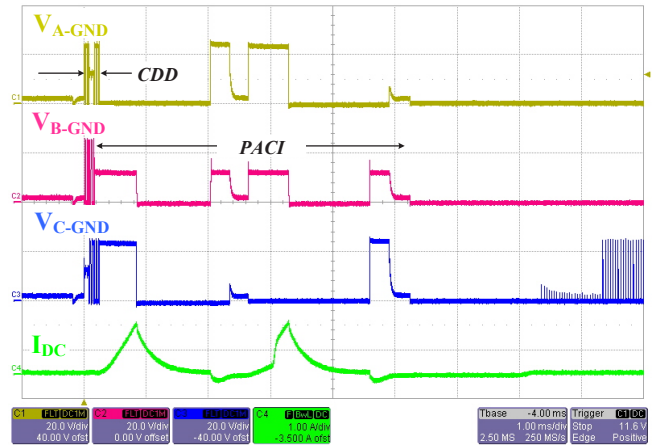


Figure 14: 2-Pulse IPD Waveforms (With DC Link Current)

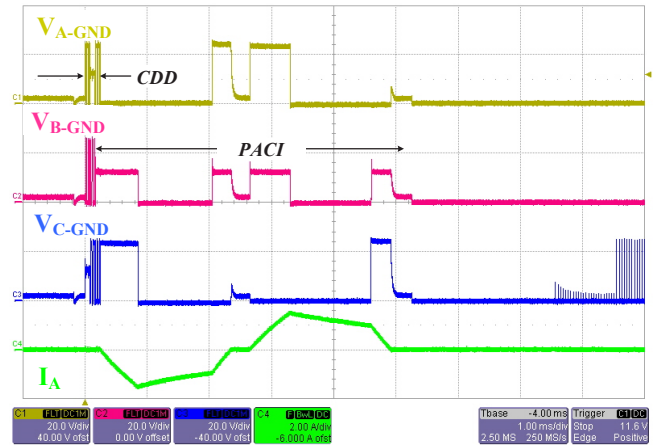


Figure 15: 2-Pulse IPD Waveforms (With Phase Current)

The 2-pulse IPD procedure is summarized below. Here, Steps 1 through 4 correspond to the CDD stage, and Steps 5 through 7 correspond to the PACI stage.

1. Drive the first pair (AB) of phase voltages, and measure the floating voltage (C).
2. Drive the second pair (AC) of phase voltages, and measure the floating voltage (B).

3. Drive the third pair (BC) of phase voltages, and measure the floating voltage (A).
4. Determine the possible sector location of the rotor.
5. Drive the current in the first direction, and measure the time to reach the threshold.
6. Drive the current in second direction, and measure the time to reach the threshold.
7. Compare the times obtained in Steps 5 and 6, and determine the rotor position.

The 2-pulse IPD has various advantages over the conventional 6-pulse IPD technique.

- **Quiet Operation:** 2-pulse IPD is relatively quiet and does not generate any significant acoustic noise or vibration because of the higher switching frequency of 25 kHz.
- **Detection Time:** Rotor position detection time is less than that of the 6-pulse IPD due to the higher switching frequency.
- **Position Resolution:** 2-pulse IPD has a finer position resolution of 30 degrees as compared to 60 degrees with the 6-pulse IPD.
- **Torque:** 2-pulse IPD generates lower torque compared to the 6-pulse IPD.
- **Maximum Torque:** The maximum torque in 6-pulse IPD is proportional to $\sin(60/2) = 0.5$, and in 2-pulse IPD is proportional to $\sin(30/2) = 0.258$. Hence, the maximum torque during IPD for 2-pulse IPD is almost half that of the 6-pulse IPD.
- **Accuracy:** 2-pulse IPD provides better accuracy because the PACI technique compares two sectors that can be either aligned or opposed.
- **Tolerance:** 2-pulse IPD provides better tolerances at the unbalanced windings because two pulses are applied and the unbalanced motor winding error is canceled out.

Slight-Move Algorithm

The 6-pulse and 2-pulse IPD algorithms ensure that the rotor does not move during detection; however, the time duration for the detection may not be acceptable for applications where slight movement is acceptable but fast startup is required, such as seat cooling fans. For such applications, slight-move algorithms can be used.

In a slight-move algorithm, asymmetrical (duty \neq 50%) complementary pulses are applied to the motor phases.

During the asymmetrical application of duty, the average current is not zero, and a small DC offset is generated. This DC offset current generates torque that slightly moves the rotor. The voltage of the floating phase is monitored to detect the zero-crossing.

As shown in Figure 16, once Sectors S0 and S6 are detected by the CDD algorithm, asymmetrical duty is applied to Phase BC (Phase B as 45% and Phase C as 55%), and the back-EMF of the floating phase (Phase A) is monitored. As the back-EMF and the $V_{bb}/2$ signal become equal, the rotor will become aligned in either the P1 or the P2 position, as shown in Figure 16. The P1 and P2 positions are 90 degrees apart. The floating phase back-EMF reaching the $V_{bb}/2$ level is shown in Figure 17, and the zoomed waveforms of the asymmetrical CDD are shown in Figure 18.

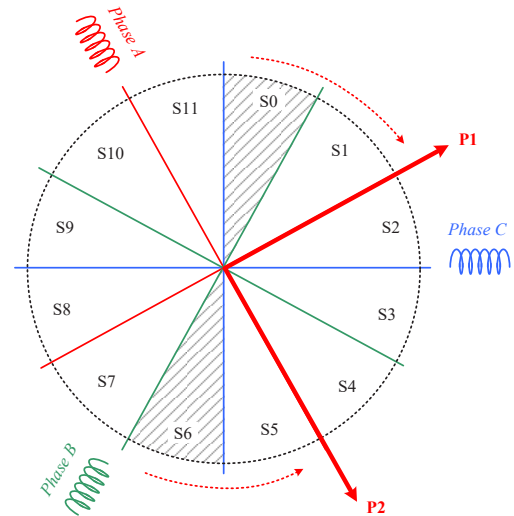


Figure 16: Slight-Move Position Alignment

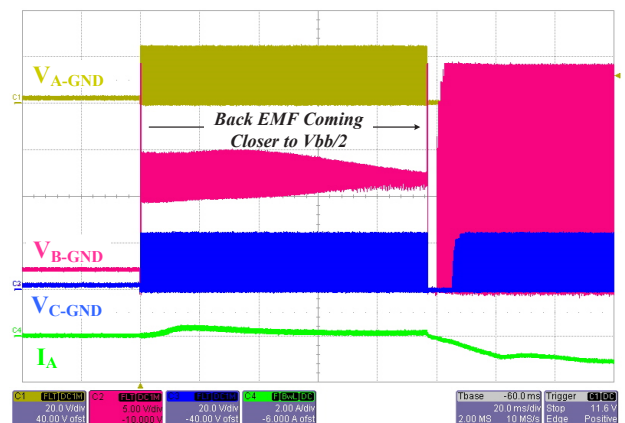


Figure 17: Back-EMF Reaching $V_{bb}/2$

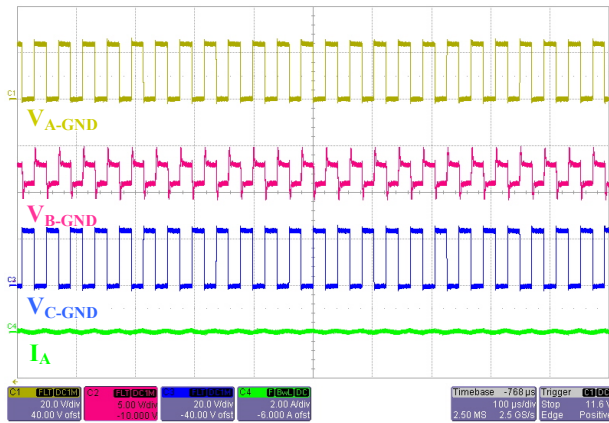


Figure 18: Zoomed Waveforms (Overall)

Once the asymmetrical CDD is complete, if the rotor position is aligned in Sector S0, the rotor would have moved to the P1 position; else, if the rotor position is in Sector S6, the rotor would have moved to the P2 position. Now, the final position is determined by driving Phases A and B or Phases A and C with complementary signals (partial CDD method).

The slight-move procedure is summarized below. Here, Steps 1 through 4 correspond to the CDD algorithm, Steps 5 through 7 correspond to the asymmetrical CDD algorithm, and Steps 8 through 9 correspond to the partial CDD algorithm.

1. Drive the first pair (AB) of phase voltages, and measure the floating voltage (C).
2. Drive the second pair (AC) of phase voltages, and measure the floating voltage (B).
3. Drive the third pair (BC) of phase voltages, and measure the floating voltage (A).
4. Determine the possible sector for the location of the rotor.
5. Apply torque to the motor with drive signals that do not have 50% duty, i.e., asymmetrical pulses (e.g., Phase BC).
6. Measure the floating phase voltage (e.g., Phase A), and compare the measured value to the threshold.
7. When the threshold levels are met, remove the asymmetrical pulses.
8. Drive any pair (AC/AB) of phase voltages, and measure the floating voltage.
9. Determine the actual sector based on the floating phase voltage.

AMT49406 CONFIGURATION

The AMT49406 device offers configuration of the startup-related parameters provided in this section.

- **Startup Mode:** This setting is used for the selection of either of the four starting modes:
 - A. Align and Go Startup Mode
 - B. 6-Pulse IPD Startup Mode
 - C. 2-Pulse IPD Startup Mode
 - D. Slight Move Startup Mode
- **Startup Current:** AMT49406 provides seven options for the startup current. The motor phase current will gradually increase to the programmed value based on the acceleration parameter. The startup current is programmed as a multiplication of rated current with the following options:

A. 1/4×	E. 3/4×
B. 3/8×	F. 7/8×
C. 1/2×	G. 1×
D. 5/8×	

For comparison, two different startup currents (i.e., 1/4× and 3/4×) are shown in Figure 19 and Figure 20, respectively.

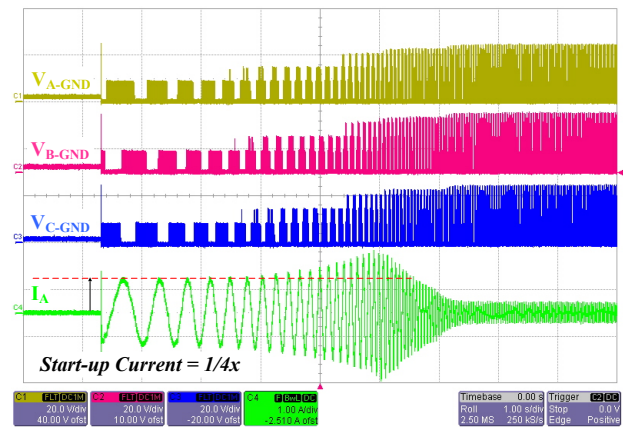


Figure 19: Startup Waveform with 1/4x Startup Current

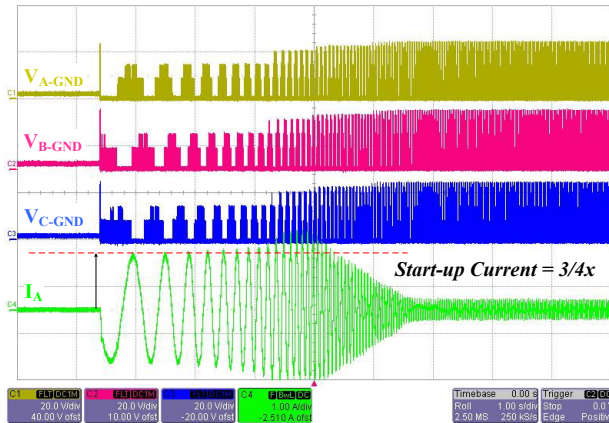


Figure 20: Startup Waveform with 3/4x Startup Current

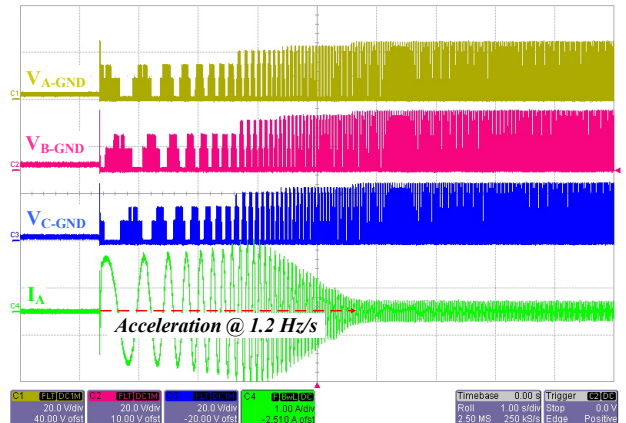


Figure 22: Startup Waveform with 3/4x Startup Current

- **Acceleration at Startup and Acceleration Range:** A wide range of acceleration parameters are provided in the AMT49406 device: higher acceleration values allow faster increases in motor speed, which can lead to startup failures; whereas lower acceleration values at startup improve the startup reliability, but can result in noise during startup. Hence, selection of the effective acceleration parameter becomes very important for smooth and reliable startup. Acceleration is set with two acceleration range settings as follows:

- 0 to 12.75 Hz/s with 0.8 Hz/s resolution
- 0 to 816 Hz/s with 51.2 Hz/s resolution

For comparison, two different accelerations (i.e., 0.6 Hz/s and 1.2 Hz/s) are shown in Figure 21 and Figure 22, respectively.

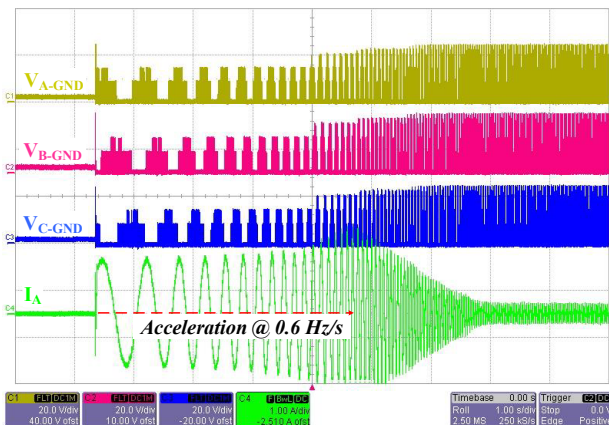


Figure 21: Startup Waveform with 3/4x Startup Current

- **Speed Control:** This parameter defines the speed control technique of the AMT49406 driver. Two options are available:
 - Open-Loop: In open-loop speed control mode, the applied signal to the speed pin (or I2C speed register) is the input duty to the motor driver. The “Open-Loop Acceleration and Deceleration Buffer” parameters are used for tuning the transient response.
 - Closed-Loop: In closed-loop speed control mode, the applied signal to the speed pin (or I2C speed register) is the percentage of rated speed to the motor driver. The “Speed Response Time” constant parameter is used for tuning the dynamic performance.
- **Open-Loop Acceleration and Deceleration Buffer:** The acceleration and deceleration buffer only affects the “Open-Loop Speed Control” mode. Use of the default setting is recommended unless the dynamic performance of the system is not satisfactory. If a faster dynamic response is desired (and the rotor inertia is low), fast or no buffer can be chosen. However, for applications that require a high-inertia motor (e.g., ceiling fans), a slow buffer is recommended. A fast buffer with a slow system may cause a lock-detect mistrigger. This acceleration and deceleration buffer can be set to one of four options:
 - None (No Buffer)
 - Fast
 - Medium
 - Slow

The dynamic response with change in duty from 50% to 100% for the slow and medium acceleration/deceleration buffer settings are shown in Figure 23 and Figure 24, respectively. As shown in these figures, the slow buffer shows a slow dynamic response, but also has lower transients compared to the medium buffer setting.

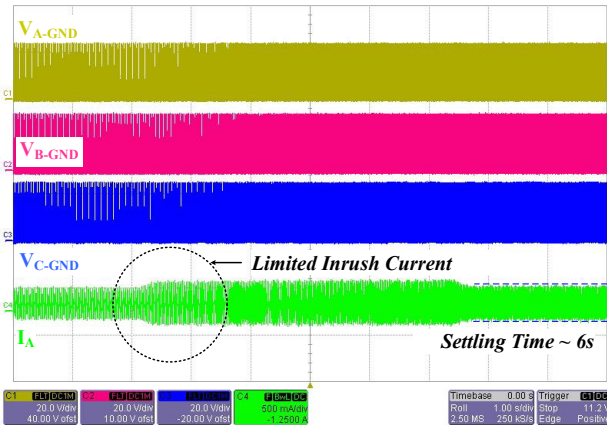


Figure 23: Speed Change with Slow Buffer Setting

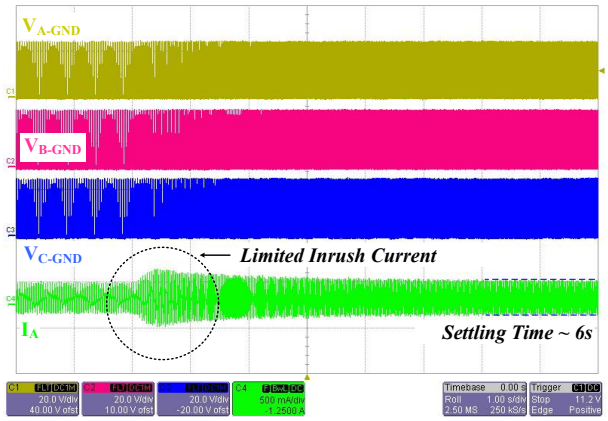


Figure 25: Speed Change with Higher Speed Time Constant (Slower Response)

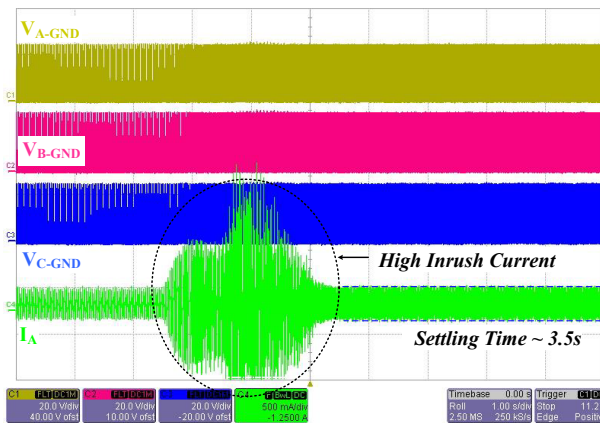


Figure 24: Speed Change with Medium Buffer Setting

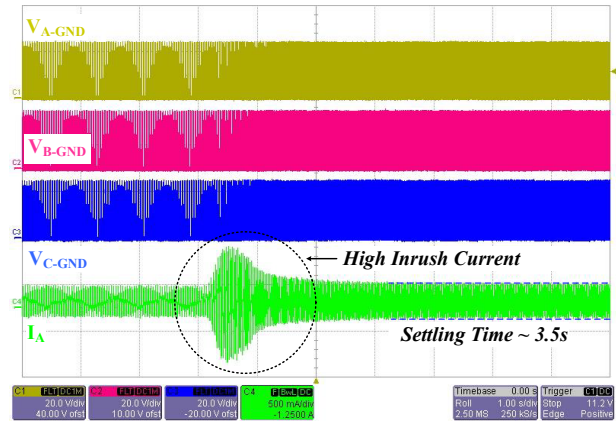


Figure 26: Speed Change with Lower Speed Time Constant (Faster Response)

- Speed Response Time Constant:** The speed response time constant only affects the "Closed-Loop Speed Control" mode. This is effectively the time constant of the speed controller: higher values result in a slower transient response but lower current transients; whereas lower values result in faster dynamic behavior but with the cost of higher transient current. Hence, this parameter can be tuned based on the dynamic performance requirement and the margins available for the current overshoot. The speed response time constant can be adjusted from 0.07 to 2.8 seconds with average resolution of 0.65 seconds.

The dynamic responses with change in speed demand from 50% to 100% for a 1 second and a 0.53 second speed demand response time setting are shown in Figure 25 and Figure 26, respectively. As shown in these figures, the higher speed time constant shows a slow dynamic response and limited inrush current, whereas the lower response time setting shows a higher inrush current with lower setting time.

- IPD Current Threshold:** This parameter defines the peak current threshold for the IPD algorithms (i.e., 2-pulse IPD and 6-pulse IPD). The IPD current threshold needs to be set high enough for reliable motor startup, but as low as possible to minimize acoustic noise during startup. The waveform of the 6-pulse IPD algorithm with IPD current threshold set to 1.2 A is shown in Figure 27.

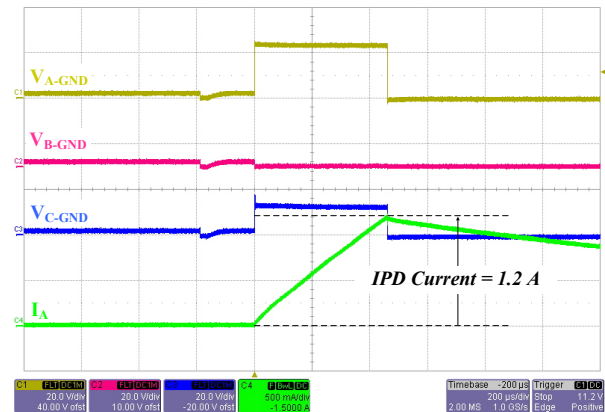


Figure 27: IPD Current Threshold

- **Slight-Move Control Demand:** This parameter defines the amplitude demand in slight-move algorithm mode. If the demand value is set too high, the motor can cause a severe startup oscillation. However, if the demand value is too low, the motor can cause startup failure.

The impact of slight-move control demand at 5.6% and 18% is shown in Figure 28 and Figure 29, respectively. As shown in Figure 24, due to the high duty demand, there is a significant rise in the peak current.

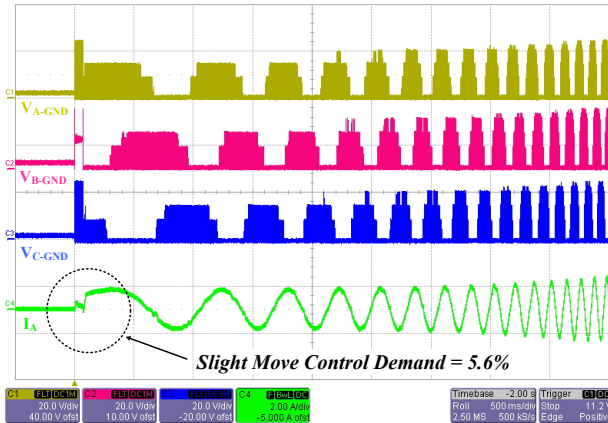


Figure 28: Slight-Move Control Demand @ 5.6%

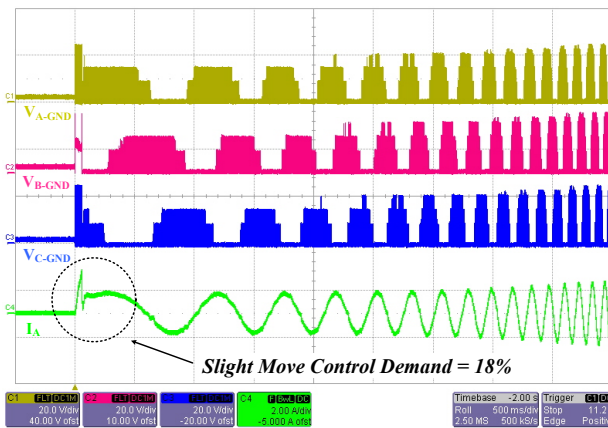


Figure 29: Slight-Move Control Demand @ 18%

- **Open Drive—Stepper Mode:** This mode is a debug option that keeps the open-loop startup mode always enabled and prevents the AMT49406 device from entering closed-loop control. If the motor is not spinning, this mode allows the motor to spin slowly in an open loop (e.g., the rated speed is allowed to be set to a lower value); the problem is associated with the proportional and integral gains of the position observer.
- **Current Control:** This mode is also a debug option that disables the current limit and the accelerate/decelerate

buffer. In this mode, the speed command will always be the same as the speed demand. This will eliminate any issues related to current limit; however, precaution should be taken to ensure that motor current does not exceed the thermal breakage limits.

- **Delay Start:** The “Delay Start” parameter extends the delay between the signal on the surge protection device (SPD) terminal and motor startup to 100 ms. This option is used if the voltage on V_{bb} is not stable within 25 ms after a start signal is applied to the SPD terminal. In many application scenarios, the SPD terminal is biased such that the motor will begin to run immediately when supply voltage (V_{bb}) is applied, and the supply slew rate is slow. If the supply slew rate is not stable within 25 ms of application of the start signal, the “Delay Start” option can be set, which extends the delay between the signal on the SPD terminal and motor startup time to 100 ms. Note that, if this option is enabled, the 100 ms delay is always present and is not limited to the application of supply voltage.
- **Open Window:** This feature is a debug option that allows the user to adjust parameters (such as motor inductance) for the best efficiency. As the name suggests, when this option enabled during the phase current decay to zero, a small window is opened that allows the phase terminal to monitor the back-EMF, which is needed because the phase will be floating, as shown in Figure 30. This back-EMF can be compared with the $V_{bb}/2$ voltage reference to determine if the current is leading or lagging, and parameters such as inductance can be adjusted accordingly. An explanation of this phenomenon follows.

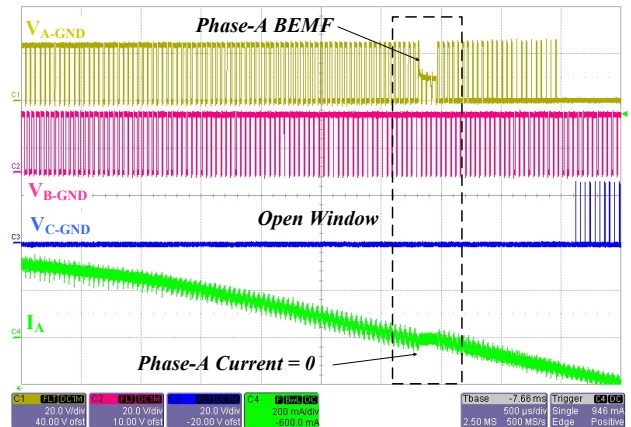


Figure 30: Open Window Operation

During the motor operation, as shown in Figure 9, the neutral point voltage (V_{CT}) is calculated as shown in Equation 1 and Equation 2. By adding these equations and rearranging, the

voltage at floating phase C (V_C) is written as:

Equation 8:

$$V_C = V_{CT} = \frac{V_{bb}}{2} + \frac{i_{ab}}{2} \times (R_b - R_a) + \frac{(L_b - L_a)}{2} \frac{d}{dt} (i_{ab}) - \frac{(e_{an} + e_{bn})}{2}.$$

Considering a balanced resistor and ignoring the small difference in the per-phase inductance, Equation 8 can be rearranged as:

Equation 9:

$$V_C = V_{CT} = \frac{V_{bb}}{2} - \frac{(e_{an} + e_{bn})}{2}.$$

For a three-phase equilibrium system, ignoring the harmonic content, the sum of per-phase back-EMF voltages is zero, written as:

Equation 10:

$$e_{an} + e_{bn} + e_{cn} = 0.$$

Combining Equation 9 and Equation 10 produces:

Equation 11:

$$V_C = V_{CT} = \frac{V_{bb}}{2} + \frac{e_{cn}}{2}.$$

Hence, from Equation 11, it is shown that the floating phase voltage is merely dependent on the back-EMF voltage superposition on the $V_{bb}/2$ voltage.

For the ideal condition, the back-EMF and phase current are expected to be aligned current, as shown in Figure 31 (black solid and dotted waveforms) for the maximum output power. However, due to inaccuracy in the value of inductance used in the FOC algorithm, the actual back-EMF can be either lagging (BEMF-1) or leading (BEMF-2), as shown in Figure 31. This back-EMF voltage is either added (BEMF-1) or subtracted (BEMF-2) with the $V_{bb}/2$ signal to constitute the floating voltage (Equation 11).

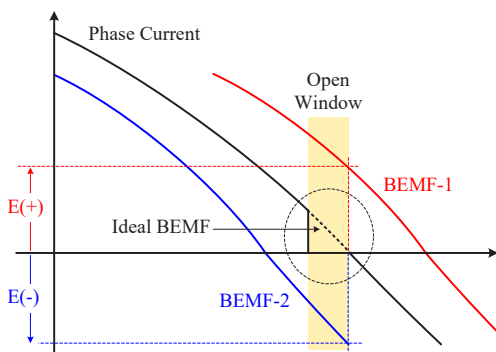


Figure 31: Phase Lead and Lag Behavior

This floating phase voltage can be classified as either the phase-lagging back-EMF or the phase-leading back-EMF as follows:

- A. For the phase-lagging back-EMF (BEMF-1), the floating phase voltage exceeds $V_{bb}/2$, which suggests the phase-lagging component (inductive impedance, X_L) is not sufficient (because current is leading the back-EMF); thus, the inductance value is insufficient, and the inductance parameter must be increased.
 - B. For the phase-leading back-EMF (BEMF-2), the floating phase voltage is lower than $V_{bb}/2$, which suggests that the phase-lagging component (X_L) is lower; therefore, the value of inductance has been set at some higher value, and the value of the inductance parameter must be decreased.
- **Soft-On and Soft-Off:** The soft-on and soft-off (SOSO) feature gradually increases the current to the motor upon receipt of the "on" command (windmill condition), and gradually reduces the current from the motor upon receipt of the "off" command, reducing the acoustic noise and operating the motor smoothly. The SOSO feature can be enabled or disabled independently.

For comparison, the functionality of the SOSO feature when disabled and enabled is shown in Figure 32 and Figure 33, respectively. As shown in Figure 32, as soon as the "PWM off" command is issued, the switches are turned off and the current becomes zero, showing a hard current stop. Also, as soon as the motor is restarted (the motor is still running in this scenario), if the soft-on feature is disabled, a huge inrush current will be drawn. However, as shown in Figure 33, in soft-off poweroff, the current is not decayed to zero instantaneously, and the PWM duty is reduced gradually. As the motor is still running during the current decay, the PWM is applied again. Because the soft-on feature is enabled, this inrush current is limited.

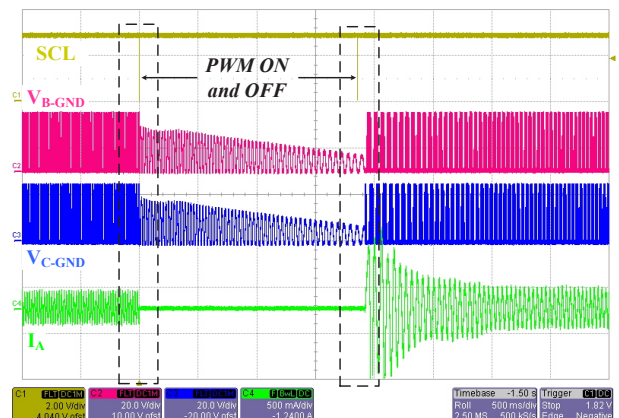


Figure 32: Soft-On and Soft-Off are Disabled

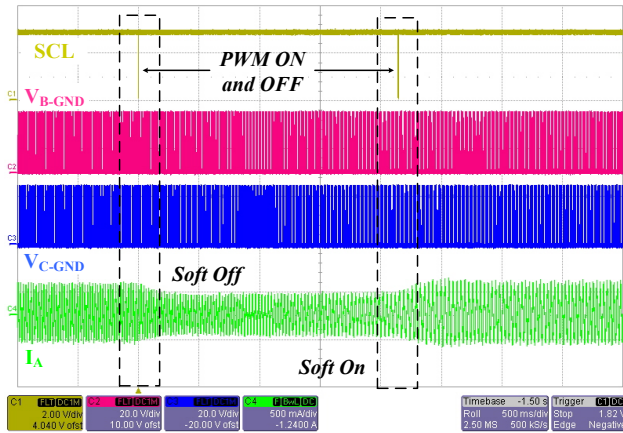


Figure 33: Soft-On and Soft-Off are Enabled

The impact of the soft-on feature is clearly shown in Figure 34, (here, the soft-off feature is disabled). The starting inrush current is almost eliminated as compared to inrush current in Figure 32 (where soft-on is disabled).

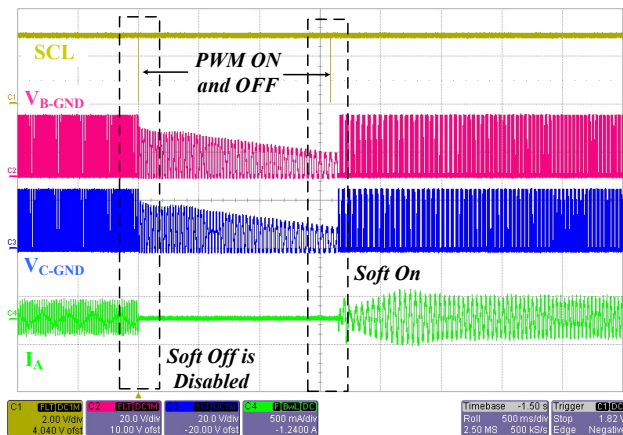


Figure 34: Soft-On is Enabled and Soft-Off is Disabled

- **First Cycle Speed:** As the name suggests, the first cycle speed is the frequency of the first cycle of the startup. To achieve a faster startup, this parameter is increased. This parameter can be configured in any of four options:
 - A. 0.55 Hz
 - B. 1.1 Hz
 - C. 2.2 Hz
 - D. 4.4 Hz

For comparison, two different first cycles (i.e., 2.2 Hz and 4.4 Hz) are shown in Figure 35 and Figure 36, respectively. As shown in these figures, if the first cycle frequency is low, the overall startup time increases.

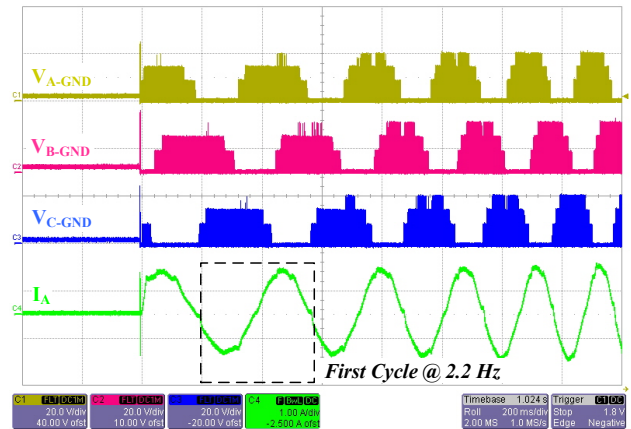


Figure 35: First Cycle at 2.2 Hz

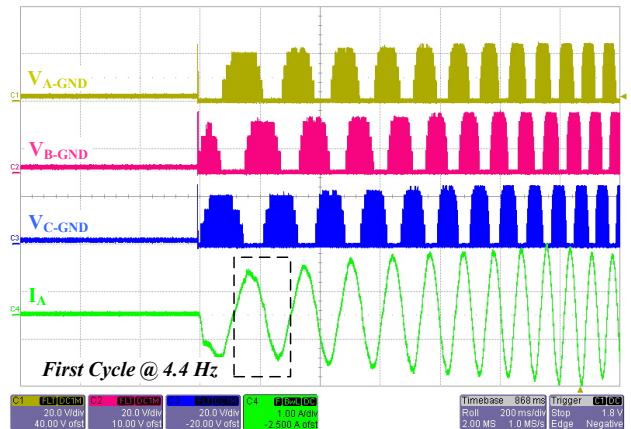


Figure 36: First Cycle at 4.4 Hz

- **Exit Windmill Threshold:** This parameter sets the exit threshold for reverse windmill operation. During the reverse windmilling operation, if the reverse windmilling period (i.e., the period of the frequency generator, FG, signal) is higher than the set “Exit Windmill Threshold” value, the IC exits windmilling operation and applies the brake to restart the motor in the set direction. This parameter can be configured in any of four options:
 - A. 320 ms
 - B. 160 ms
 - C. 80 ms
 - D. 40 ms
- **Startup During Reverse Windmilling:** This setting determines the startup procedure of the motor during the reverse-windmilling operation as follows:
 - A. **Wait until motor stops:** The AMT49406 driver will wait for the speed to drop below the threshold set by “Exit Windmill Threshold”; then it will apply the brake.

B. **If the motor does not stop, attempt startup after 5 seconds:** This option is used if the possibility exists for an external force to prevent the motor from coming to a complete halt and if the motor speed never falls below the "Exit Windmill Threshold". In such application, this setting allows the motor to brake and attempt restart after 5 seconds.

Note: During the braking operation, if the brake mode parameter is set to "Brake When Safe", the motor will only brake when it is safe.

IPD PERFORMANCE TESTING

The AMT49406 graphical user interface (GUI) provides an IPD performance testing page used to test the performance of the IPD algorithm and to tune the motor startup parameters. This test is applied to the 2-pulse IPD, 6-pulse IPD, and slight-move algorithms. The IPD testing configurations include settings for two stages as follows:

- A. Stage 1: Applicable to the 2-pulse IPD and slight-move algorithms.
- B. Stages 1 & 2: Applicable to the 2-pulse IPD and 6-pulse IPD algorithms.

The testing procedure and explanations of the significance of various settings used for IPD testing are as follows:

1. Go to the IPD page, select the IPD test stage, enable "Continuously Read Angle", and push "Toggle Run/Stop" to start driving.

The motor will not spin, but will make some noise due to the application of the IPD signals.

2. Manually rotate the rotor of motor slowly.

The detected motor position will be shown in the "Clock" plot and the "X-Y" plot of the IPD page.

3. Observe the output and follow the following guidelines as relevant to the scenario:

- If "Stage 1" is selected, the output will successively step up from 45 degrees to 195 degrees, then back to 45 degrees, if spun in the target direction. If spun in the opposite direction, the output will successively step down from 195 degrees to 45 degrees, then back to 195 degrees, as shown in Figure 37.
- If "Stages 1 & 2" is selected, the output will successively step up from 15 degrees to 345 degrees, then back to 15 degrees, if spun in target direction. If spun in the opposite direction, the output will successively step down from 345 degrees to 15 degrees, then back to 345 degrees, as shown in Figure 38.

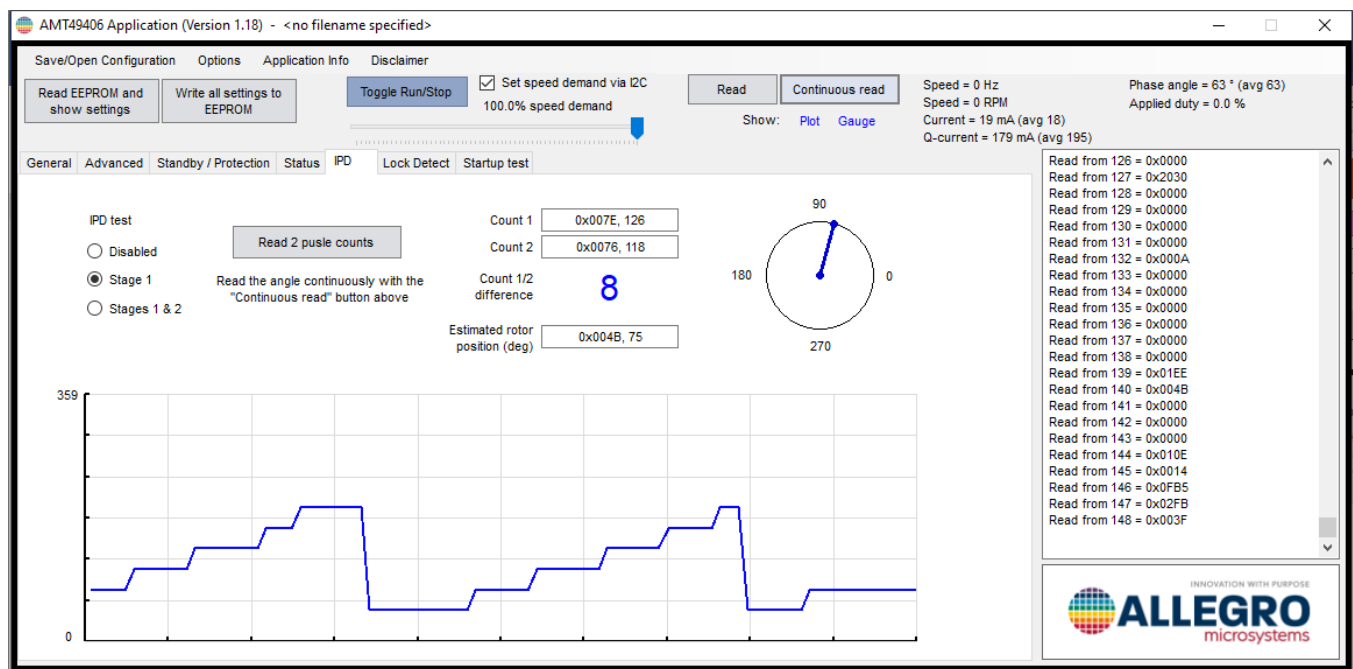


Figure 37: "Stage 1" IPD Testing

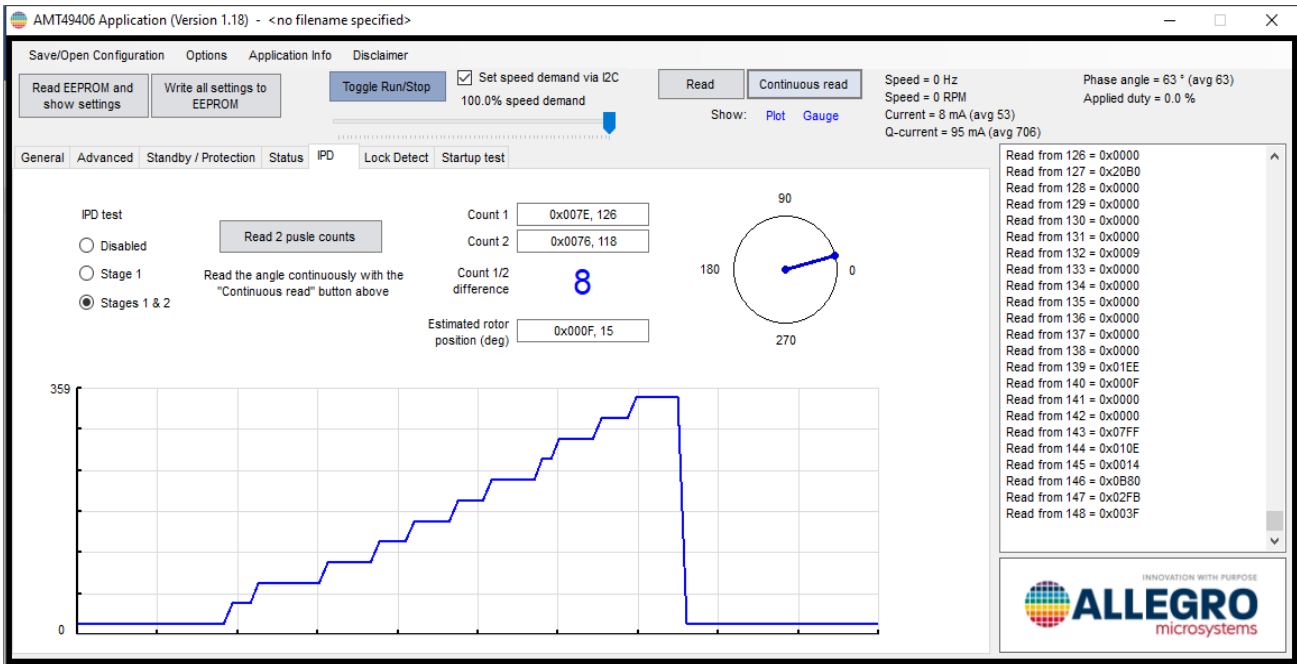


Figure 38: “Stages 1 & 2” IPD Testing

4. If using the “2-Pulse IPD” or “Stages 1 & 2” option, press the “Read 2 Pulse Counts” button.

“Counter 1” and “Counter 2” will display the widths of the two pulses, and the difference will be calculated. The difference of the counter values is expected to be above 3 or below -3.

Note that “Counter 1” and “Counter 2” apply only to the “2-Pulse IPD” and “Stages 1 & 2” options.

5. Observe the motor angle steps.
 - If the detected motor angle steps are not successive in “Stage 1” while slowly rotating the rotor (for example, if the angle jumps from 45 degrees to 135 degrees, then back to 75 degrees), the “2-Pulse IPD” and “Slight-Move” modes are not proper startup modes for this motor. In this scenario, use either the “6-Pulse IPD” or “Align and Go” algorithms.
 - If “Stage 1” is good (or if “6-pulse IPD” is selected) and the detected motor angle steps are not successive in

“Stages 1 & 2” while slowly rotating the rotor (e.g., angle jumping from 45 degrees to 225 degrees, then back to 45 degrees—especially jumping back and forth around 180 degrees), increase the “IPD current threshold”.

Note that It is normal for the result to move one step (30 degrees) back and forth. This variance will not affect the startup reliability, as shown in Figure 39.



Figure 39: Back-and-Forth Movement of 30 degrees

- If “Stages 1 & 2” is good but the difference calculated between the widths of Pulse 1 and Pulse 2 is only ± 0 , 1, or 2, increase the “IPD Current Threshold” to reach a counter magnitude difference greater than 3.

CONCLUSION

This application information has explored various startup techniques available in the sensorless FOC BLDC motor driver AMT49406. A detailed description of the various startup techniques with a key focus on the application viability and limitations, and details of the operating principle have been presented. Newly developed 2-pulse IPD and the slight-move algorithms have been presented that achieve a faster startup than the conventional techniques. Various configuration parameters available in the AMT49406 device have been explained in detail, including the impact of those parameters during startup. Finally, an IPD window for tuning the AMT49406 parameters has been explained.

With very high integration of startup features like the soft-on and soft-off, nonreverse fast startup techniques like the 2-pulse IPD, the flexibility to select numerous parameters selection, and the ease of tuning the parameters for various applications, combined with the code-free sensorless field-control algorithm make the AMT49406 a very versatile device in the market.

REFERENCES

- [1] Allegro MicroSystems Launches QuietMotion Family of Code-Free FOC Sensorless BLDC Fan Drivers, Allegro Newsroom, Jan. 2019; <https://www.allegromicro.com/en/about-allegro/news-room/2019/quiet-motion-press-release>.
- [2] AMT49406: 50 V Code-Free FOC BLDC Motor Controller, Allegro MicroSystems datasheet, MCO-0000542, Rev. 2, June 2020; <https://www.allegromicro.com/products/motor-drivers/bldc-drivers/amt49406>.
- [3] AMT49406 Configuration Procedure, Allegro Microsystems Application Information, Rev. 6, Jan 2019; https://registration.allegromicro.com/downloads/AMT49406%2FpartSupportFile%2FAMT49406_Configuration_Procedure_v06.pdf (login to the Allegro Software Portal at <https://registration.allegromicro.com/login> is required).
- [4] Yisong Lu and Lyndon Ambruson, Determining Motor Position with Complimentary Drive and Detect and Slight Move, US Patent, US 10116243 B2, Oct. 2018.

Revision History

Number	Date	Description	Responsibility
-	June 13, 2022	Initial release	V. Bist, S. Wekhande

Copyright 2022, Allegro MicroSystems.

The information contained in this document does not constitute any representation, warranty, assurance, guaranty, or inducement by Allegro to the customer with respect to the subject matter of this document. The information being provided does not guarantee that a process based on this information will be reliable, or that Allegro has explored all of the possible failure modes. It is the customer's responsibility to do sufficient qualification testing of the final product to ensure that it is reliable and meets all design requirements.

Copies of this document are considered uncontrolled documents.